Stochastic Resonance in a Single-Ion Nonlinear Mechanical Oscillator

Tai-Hao Cui(崔太豪)[1,2†], Ji Li(李冀)[3†], Quan Yuan(袁泉)[1,2†], Ya-Qi Wei(魏雅琪)[4], Shuang-Qing Dai(戴双晴)[1,2], Pei-Dong Li(李沛东)[1,2], Fei Zhou(周飞)[1,3], Jian-Qi Zhang(张建奇)[1*], Liang Chen(陈亮)[1,3*], and Mang Feng(冯芒)[1,3,5*]

[1]*State Key Laboratory of Magnetic Resonance and Atomic and Molecular Physics, Wuhan Institute of Physics and Mathematics, Innovation Academy of Precision Measurement Science and Technology, Chinese Academy of Sciences, Wuhan 430071, China*
[2]*University of Chinese Academy of Sciences, Beijing 100049, China*
[3]*Research Center for Quantum Precision Measurement, Guangzhou Institute of Industry Technology, Guangzhou 511458, China*
[4]*Laboratory of Quantum Science and Engineering, South China University of Technology, Guangzhou 510641, China*
[5]*Department of Physics, Zhejiang Normal University, Jinhua 321004, China*

(Received 7 April 2023; accepted manuscript online 20 July 2023)

Stochastic resonance is a counterintuitive phenomenon amplifying the weak periodic signal by application of external noise. We demonstrate the enhancement of a weak periodic signal by stochastic resonance in a trapped-ion oscillator when the oscillator is excited to the nonlinear regime and subject to an appropriate noise. Under the full control of the radio-frequency drive voltage, this amplification originates from the nonlinearity due to asymmetry of the trapping potential, which can be described by a forced Duffing oscillator model. Our scheme and results provide an interesting possibility to make use of controllable nonlinearity in the trapped ion, and pave the way toward a practical atomic sensor for sensitively detecting weak periodic signals from real noisy environment.

DOI: 10.1088/0256-307X/40/8/080501

Motion of trapped ions confined in a quadruple electromagnetic trap is highly controllable, usually stabilized at equilibrium positions, i.e., within the linear regime.[1] It allows manipulation of the ions to explore new physics at atomic levels and even at the quantum mechanics level.[2] In contrast, if they are driven away from the equilibrium positions to the nonlinear regime, the ions will suffer from motional heating and thereby be instable due to experiencing high-order multipole potentials, such as hexapole and octopole potentials.[1] However, if controllable, the nonlinearity of the trapped ion can be useful, for example, to achieve trapped-ion phononic lasing[3–5] and to work for resonance detection in trapped-ion mass spectrometry.[6,7] Moreover, a single trapped ion behaves like a Duffing oscillator when driven to the nonlinear regime,[8] which may be used for ultraprecision measurement beyond the quantum standard limit.[9]

In this work, we focus on the nonlinear dynamics of a single trapped ion confined in a surface-electrode trap (SET), and demonstrate the enhancement of weak periodic signals from the noise making use of the technique of stochastic resonance. Noises are unavoidable in real physical measurements. Distinguishing and even extracting information from noisy environment are practically challenging in information processing. In what follows, we exemplify the white Gaussian noise, which features flat power spectrum properties with instantaneous values obeying Gaussian distribution. We show below how to enhance the weak signal from this noise by considering signals with different strengths.

Stochastic resonance is a counterintuitive phenomenon that has been attracting growing attention for years.[10] It occurs in nonlinear systems whereby the weak periodic signal can be amplified with addition of noises. Thus the system undergoes a resonance-like response with the help of the noises. Stochastic resonance has been observed in various macroscopic systems, such as the cyclic recurrence of ice ages,[11] the receptors in crickets[12] and crayfish,[13] as well as some artificial physical devices.[14–16] Recently, stochastic resonance was applied to microscopic systems[17–22] to show the possibility of phase noise metrology[23] or coherent signal transmission.[24]

The unique observation in the present work due to stochastic resonance is from the strong asymmetry in the SET, which originates from different layouts and fabrication characteristics.[25] When we stimulate the axial (i.e., z-axis) vibration of the trapped-ion oscillator by an rf drive, the motion of the trapped ion turns gradually away from the linear regime, which is reflected by the hysteresis behavior observed in the sweep of the drive frequency back and forth with respect to the z-axis vibrational frequency. This indicates the occurrence of the bistable state, a typical nonlinear phenomenon that can be fully described by complicated Duffing oscillators. As clarified below, we show in the bistability regime that the weak periodic sig-

†These authors contributed equally to this work.
*Corresponding authors. Email: changjianqi@gmail.com; liangchen@wipm.ac.cn; mangfeng@wipm.ac.cn
© 2023 Chinese Physical Society and IOP Publishing Ltd

nals can be amplified after the external noise is applied, which may be useful for fundamental physics and practical applications.

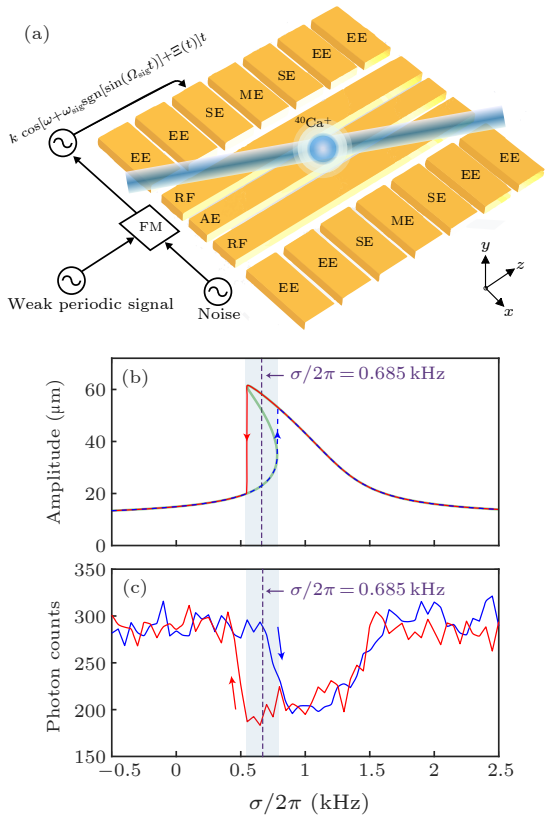

Fig. 1. Schematic of stochastic resonance by the single-ion nonlinear mechanical oscillator. (a) Schematic of the experimental setup. The ion trap is an SET which confines a single ion under a red-detuned laser irradiation. The top view of the SET demonstrates the seven pairs of side electrodes, two rf electrodes and an axial electrode (AE). The symbols on the side electrodes are for convenience of discussion, where EE, SE, and MS represent, respectively, the end electrode, side-control electrode, and middle electrode. The drive, the external noise, and the weak periodic signal are input from the SE. FM: Frequency modulation. The image of the ion is observed by the electron-multiplying charge-coupled device (EMCCD) and we record the fluorescence from the spontaneous emission by the photomultiplier tube (PMT). For clarity of plotting, both EMCCD and PMT are not shown here. [(b), (c)] The theoretical simulated and experimental observed hysteresis loop, as highlighted by the shade: (b) the amplitude variation of the single-ion oscillator with respect to the detuning $\sigma = (\omega - \omega_z)$, based on the numerical solution of Eq. (1) with $k = 1.5521 \times 10^7$ m·Hz^2, $\alpha = -6.2675 \times 10^4$ Hz^2/m^2, $\mu = 0.1055$ Hz, (c) the photon counts experimentally by sweeping the drive frequency ω back and forth with respect to ω_z, where the blue (red) line represents the positive (negative) scan, as labeled by the arrows, and the central drive frequency $\sigma/2\pi = 0.685$ kHz is marked by a vertical dashed line. The scan step is 0.05 kHz and the drive strength is 27.5 mV.

Our experiment is carried out by a single trapped $^{40}Ca^+$ ion in the SET, which is a 500-μm-scale planar trap as sketched in Fig. 1(a). This SET is similar to those employed previously by the same group [26–28] but more complicated, where the secular frequencies are $\omega_z/2\pi = 265.5$ kHz, $\omega_x/2\pi = 920.0$ kHz, and $\omega_y/2\pi = 1378.5$ kHz, with ω_z and $\omega_{x(y)}$ being the axial and radial trap frequencies, respectively. The confined ions stay stably above the surface of the SET by 500 μm.

In our experiment, we drive the ion along the z-axis for additional oscillation by a signal generated from the arbitrary waveform generator. The motion of such an ion can be described by the Duffing model as follows:

$$\ddot{\tilde{z}} + 2\mu\dot{\tilde{z}} + \omega_z^2\tilde{z} + \alpha\tilde{z}^3 = k\cos(\omega t), \tag{1}$$

where $\tilde{z}$ is the displacement of the ion from the equilibrium position, α is the nonlinear coefficient, μ is the damping coefficient due to laser cooling, and k is the amplitude of the external drive with frequency ω.

To achieve stochastic resonance, we need to find the hysteresis loop, indicating the existence of bistable states, and amplification of the weak periodic signal would be realized in the bistability regime by appropriately applying an external noise. Likewise, stochastic resonance can be understood as random jumps over the potential barrier, inducing hopping between the bistable states, which results in the amplification of the weak periodic signal. This is something like the motion of a fictive particle in a double-well potential periodically modulated in amplitude by the signal under the influence of noises. [29]

Experimentally, we have first observed the hysteresis loop by sweeping the driving frequency back and forth with respect to ω_z. We drive the ion to the nonlinear regime by the oscillating voltage with $V = 27.5$ mV, applied on one of the electrodes, i.e., SE [see Fig. 1(a)]. We slowly increase the drive frequency with scan steps of 0.05 kHz, from the detuning $\sigma/2\pi = -0.5$ kHz to 2.5 kHz (i.e., scan upward or the positive scan). When the detuning increases to be around 0.820 kHz, we observe the rapidly enlarging oscillation of the ion from the EMCCD, along with a drop in the counting number of the scattering photons recorded by the PMT. Similar behavior is also found in the negative scan from 2.5 kHz down to −0.5 kHz, while the drop occurs at $\sigma/2\pi = 0.550$ kHz, as plotted in Fig. 1(b). This observation implies the existence of the bistable state, i.e., a hysteresis loop with a width of 270 Hz. As elucidated below, we perform stochastic resonance by applying a drive signal at $\sigma/2\pi = 0.685$ kHz, which is the middle point of the bistability region, and in this case the trapped ion oscillates with a large amplitude corresponding to the small photon count in the PMT. Thus, the ion is first prepared in the oscillation state with a high amplitude.

In our experiment, both the small signal with low frequency and the external noise, as required by stochastic resonance, are introduced artificially, where the small signals are given by square waveform signals with the strength ω_{sig} and frequency Ω_{sig}, and the external noise is the white Gaussian noise with the strength ξ_{n} and bandwidth B_{n}. Both the small signal and the additional noise are applied on the SE by the frequency modulation (FM) of the drive signal. Then, Eq. (1) can be rewritten as

$$\begin{aligned}&\ddot{\tilde{z}} + 2\mu\dot{\tilde{z}} + \omega_z^2\tilde{z} + \alpha\tilde{z}^3 \\ &= k\cos[\omega + \omega_{\mathrm{sig}}\mathrm{sgn}[\sin(\Omega_{\mathrm{sig}}t)] + \Xi(t)]t,\end{aligned} \tag{2}$$

where sgn[K] is a sign function for the square waveform signal with sgn[K] = 1 in the case of $K \geq 0$, and sgn[K] = -1 otherwise. $\Xi(t)$ represents the externally applied white Gaussian noise, which follows the correlation function $\langle \Xi(t)\Xi(0)\rangle = 2\xi_n\delta(t)$ with noise strength ξ_n. For simplicity, we suppose $\Omega_{sig}/2\pi = 1$ Hz, which is much lower than the external drive frequency of $\omega/2\pi = 266.185$ kHz throughout this study.

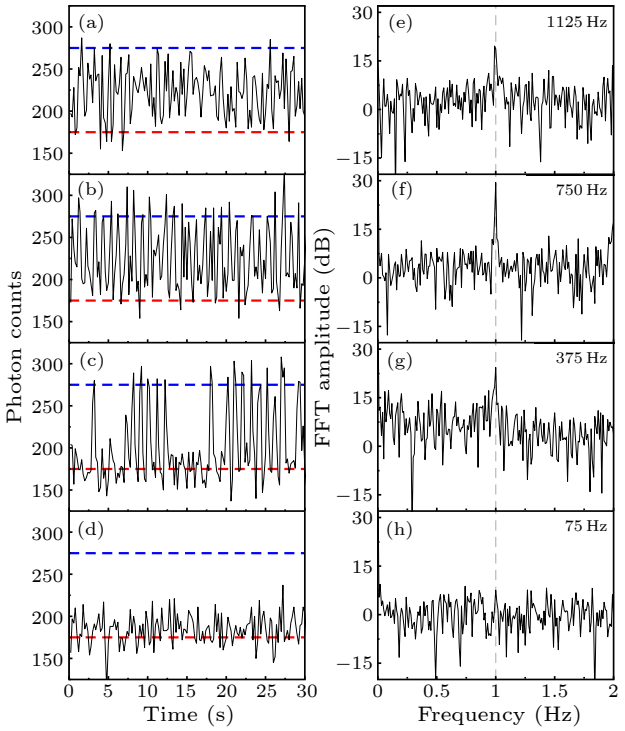

Fig. 2. The response of the system with respect to the added noise strength, where the periodic signal with the strength $\omega_{sig}/2\pi = 112.50$ Hz is of the frequency $\Omega_{sig}/2\pi = 1$ Hz, and the noise strength ξ_n, with the bandwidth $B_n = 100$ Hz, decreases from the top to the bottom panels, see the values of $\xi_n/2\pi$ labeled at the upper right corner of each right-hand side panel, 75 Hz, 375 Hz, 750 Hz, and 1125 Hz, respectively. The panels on the left show the time trace of the photon counts with the blue (red) dashed lines indicating the high (low) mean photon counts of the bistable regime shown in Fig. 1(c). The panels on the right are the corresponding FFT of the time trace results displayed in the left panels, where the vertical line means the 1 Hz frequency for guiding the eyes.

Figure 2 demonstrates the photon counts monitored in time (see the panels on the left) and the peaks in the power spectra (see the panels on the right) with enlarging strength of the noise. In the bottom panels, e.g., Fig. 2(d), since the noise is too weak to induce the hopping between the bistable states (only staying at the low photon counts of the bistability regime), the trapped ion oscillates with the large amplitude, leading to small counts of the scattering photons. Quantification of the amplified signal relies on fast Fourier transform (FFT) of the time traces. From the corresponding FFT results as plotted in the right panel, when the external noise strength is small enough, e.g., $\xi_n/2\pi = 75$ Hz in Fig. 2(h), we cannot distinguish the signal around 1 Hz from the spectra, which means no amplification of the weak signal. With the noise turning to be stronger, however, the hopping between the two states really occurs and thus we see the FFT results showing amplification of the weak periodic signal (see other panels in the right column of Fig. 2). In particular, with $\xi_n/2\pi = 750$ Hz, the hopping is synchronized with the periodic signal, which results in the best resonance effect and the maximum amplification of the weak signal. This is reflected in the photon counts oscillating fully between the two states [see Fig. 2(b)] and the highest peak of the signal at 1 Hz in the power spectra [see Fig. 2(b)]. However, when the noise is further enhanced, e.g., up to $\xi_n/2\pi = 1125$ Hz, the synchronization turns to be weaker and the corresponding signal amplification in the FFT result is lower. These observations indicate that the occurrence and effect of stochastic resonance in the bistability regime strongly depend on the noise strength.

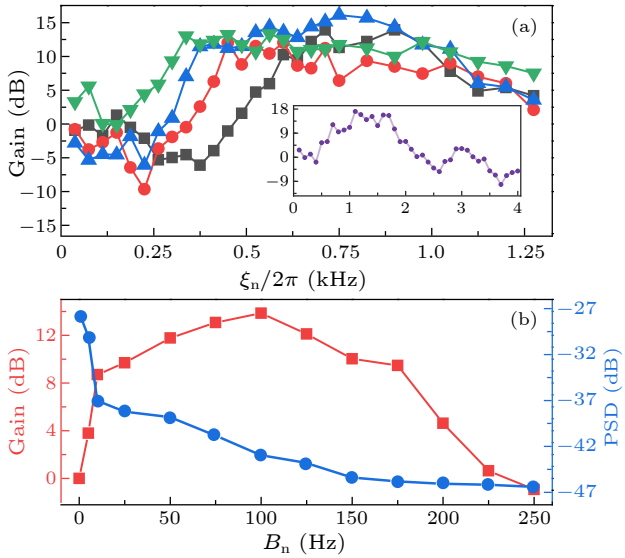

Fig. 3. (a) The gain with respect to the noise strength, where the four cases considered are with the signal strength $\omega_{sig}/2\pi = 56.25$ Hz (black squares), 75.00 Hz (red dots), 112.50 Hz (blue triangles), and 131.25 Hz (green triangles). Lines connecting the experimental data are a guide for the eyes. The inset is the numerical simulation result obtained by solving Eq. (2) in the case of $\omega_{sig}/2\pi = 75.00$ Hz. (b) Experimentally acquired gain and the noise's power spectrum density (PSD) with respect to the bandwidth of the noise, where the strength and the frequency of the weak signal are $\omega_{sig}/2\pi = 56.25$ Hz and $\Omega_{sig}/2\pi = 1$ Hz, respectively, and the noise strength is $\xi_n/2\pi = 0.75$ kHz. Red squares: gain; blue dots: PSD of the noise.

To further investigate the influence of the noise strength on stochastic resonance, we employ the signal-to-noise ratio (SNR) and the gain $G = \mathrm{SNR}(\xi_n) - \mathrm{SNR}(0)$ to quantify the amplification of the small signals by the noise, where SNR(ξ_n) is defined as the FFT results of the modulation signal in the presence of the external noise with the strength ξ_n with respect to the counterparts of the background noise. Figure 3(a) plots the relation of G to the noise strength and also shows the common characteristic, i.e., the gain value may first reduce to be negative before rising rapidly as the noise strength increases. Here

the negative gain may attribute to the suppression of the signal by the noise, when the noise is not strong enough to induce the hopping between the bistable states. This characteristic indicates that the optimal stochastic resonance depends on the suitable noise strength. In addition, the smaller signals need stronger noises for amplification, while the over-strong noise would damage the signal enhancement. Quantitatively, for the small signals under our consideration, we find that the largest gain is $G = 16\,\mathrm{dB}$ for $\omega_{\mathrm{sig}}/2\pi = 112.50\,\mathrm{Hz}$, corresponding to the amplification by 40 times.

Moreover, the gain is also relevant to the noise bandwidth, as presented in Fig. 3(b). In our case with a fixed weak periodic signal and a fixed noise strength, the gain also shows a hump-like pattern, where the gain first rises to the maximum of 13.85 dB at the bandwidth of 100 Hz and then drops to zero as the bandwidth increases to 225 Hz. To understand the underlying mechanism of this observation, we have also measured the PSD of the noise for different values of B_{n}. We find the monotone decline of the PSD with the increase of the noise bandwidth. This phenomenon indicates a threshold of the noise strength existing for the stochastic resonance, as qualified by the PSD. However, since subject to the cosine function in Eq. (2), the gain varies like a hump, instead of the monotone change. Nevertheless, the optimal hopping between the two states depends on an appropriately strong noise which can also be quantified by the PSD. In our case here, this optimal noise strength has a PSD of −42.9 dB. Furthermore, from Fig. 3(b), we may find the bandwidth range of the required gain. For example, to have the gain value larger than 3 dB, implying a double amplification, we may sweep the bandwidth, ranging from 4.9 Hz to 215 Hz.

To understand the experimental observations more deeply, we have simulated the system by Duffing nonlinear equations. Using Eq. (1) we have acquired the amplitude variation of the z-axial oscillation with respect to the driving frequency, as plotted in Fig. 1(b), whose bistability regime overlaps perfectly with that observed experimentally from the photon counts in Fig. 1(c). With Eq. (2), we have also simulated the variation of the gain with the noise strength [see the inset of Fig. 3(a)], which provides a qualitative understanding of experimentally observed humps. The underlying mechanism of the gain variation is relevant to the collaborative action of the drive, the weak signal and the noise, as denoted by the cosine function in Eq. (2).

In summary, we have experimentally demonstrated the enhancement and recognition of weak periodic signals from external noises by a trapped-ion nonlinear mechanical oscillator. Our study may be helpful for solving some particular problems of signal extractions from background noise and provides a promising way to explore practical applications of stochastic resonance at the atomic scale, including weak signal identification,[30] energy harvesting,[31] and signal extraction.[32] Moreover, our method and results are readily extended to other vibrational systems, such as microresonators, which may give deeper sight into the high-order nonlinear behavior of mechanical oscillators and the associated phenomena assisted by noises.

Acknowledgements. We acknowledge the technical support of ultrastable optical cavity and frequency stabilization from the team of Professor Qunfeng Chen. This work was supported by the Special Project for Research and Development in Key Areas of Guangdong Province (Grant No. 2020B0303300001), the National Natural Science Foundation of China (Grant Nos. U21A20434, 12074346, 12074390, 11835011, 11804375, and 11804308), and the Key Laboratory of Guangzhou for Quantum Precision Measurement (Grant No. 202201000010).

References

[1] Paul W 1990 *Rev. Mod. Phys.* **62** 531
[2] Leibfried D, Blatt R, Monroe C, and Wineland D 2003 *Rev. Mod. Phys.* **75** 281
[3] Vahala K, Herrmann M, Knunz S, Batteiger V, Saathoff G, Hänsch T W, and Udem T 2009 *Nat. Phys.* **5** 682
[4] Knunz S, Herrmann M, Batteiger V, Saathoff G, Hänsch T W, Vahala K, and Udem T 2010 *Phys. Rev. Lett.* **105** 013004
[5] Xie Y, Wan W, Wu H Y, Zhou F, Chen L, and Feng M 2013 *Phys. Rev. A* **87** 053402
[6] Drakoudis A, Snollner M, and Werth G 2006 *Int. J. Mass Spectrom.* **252** 61
[7] Makarov A A 1996 *Anal. Chem.* **68** 4257
[8] Akerman N, Kotler S, Glickman Y, Dallal Y, Keselman A, and Ozeri R 2010 *Phys. Rev. A* **82** 061402(R)
[9] Biercuk M J, Uys H, Britton J W, VanDevender A P, and Bollinger J J 2010 *Nat. Nanotech.* **5** 646
[10] Gammaitoni L, Hänggi P, Jung P, and Marchesoni F 1998 *Rev. Mod. Phys.* **70** 223
[11] Benzi R, Sutera A, and Vulpiani A 1981 *J. Phys. A* **14** L453
[12] Levin J E and Miller J P 1996 *Nature* **380** 165
[13] Douglass J K, Wilkens L, Pantazelou E, and Moss F 1993 *Nature* **365** 337
[14] Li Z P, Li C H, Xiong Z, Xu G Q, Wang Y R, Tian X, Yang X, Liu Z, Zeng Q H, Lin R Z, Li Y, Lee J K W, Ho J S, and Qiu C W 2023 *Phys. Rev. Lett.* **130** 227801
[15] Hibbs A D, Singsaas A L, Jacobs E W, Bulsara A R, Bekkedahl J J, and Moss F 1995 *J. Appl. Phys.* **77** 2582
[16] Rouse R, Han S, and Lukens J E 1995 *Appl. Phys. Lett.* **66** 108
[17] Joshi A and Xiao M 2006 *Phys. Rev. A* **74** 013817
[18] McNamara B, Wiesenfeld K, and Roy R 1988 *Phys. Rev. Lett.* **60** 2626
[19] Mompo E, Ruiz-Garcia M, Carretero M *et al.* 2021 *Phys. Rev. Lett.* **121** 086805
[20] Shao Z Z, Yin Z Z, Song H L, Liu W, Li X J, Zhu J B, Biermann K, Bonilla L L, Grahn H T, and Zhang Y H 2018 *Phys. Rev. Lett.* **121** 086806
[21] Dodda A, Oberoi A, Sebastian A, Choudhury T H, Redwing J M, and Das S 2020 *Nat. Commun.* **11** 4406
[22] Monifi F, Zhang J, Özdemir S K, Peng B, Liu Y X, Bo F, Nori F, and Yang L 2016 *Nat. Photon.* **10** 399
[23] Chowdhury A, Barbay S, Clerc M G, Robert-Philip I, and Braive R 2017 *Phys. Rev. Lett.* **119** 234101
[24] Badzey R L and Mohanty P 2005 *Nature* **437** 995
[25] House M G 2008 *Phys. Rev. A* **78** 033402
[26] Wan W, Wu H Y, Chen L, Zhou F, Gong S J, and Feng M 2014 *Phys. Rev. A* **89** 063401
[27] Li J, Yan L L, Chen L, Liu Z C, Zhou F, Zhang J Q, Yang W L, and Feng M 2019 *Phys. Rev. A* **99** 063402
[28] Liu Z C, Chen L, Li J, Zhang H, Li C, Zhou F, Su S L, Yan L L, and Feng M 2020 *Phys. Rev. A* **102** 033116
[29] Gammaitoni L, Marchesoni F, Menichella-Saetta E, and Santucci S 1989 *Phys. Rev. Lett.* **62** 349
[30] Jung P and Hänggi P 1991 *Phys. Rev. A* **44** 8032
[31] Cottone F, Vocca H, and Gammaitoni L 2009 *Phys. Rev. Lett.* **102** 080601
[32] Gu X J and Chen C Z 2019 *J. Mech. Sci. Technol.* **33** 1017